Loop Identification and Capacity Estimation of Digital Subscriber Lines with Single Ended Line Testing

Carine Neus, Wim Foubert, and Leo Van Biesen

Department of Fundamental Electricity and Instrumentation, Vrije Universiteit Brussel, Pleinlaan 2, 1050 Brussels, Belgium
{cneus,wfoubert,lvbiesen}@vub.ac.be

Abstract. Digital subscriber lines offer the possibility to deliver broadband services over the existing telephone network. Still, beforehand subscriber loops must be tested to see whether they can support high-speed data services, and at what bit rate. From the existing measurement techniques, Single Ended Line Testing is often preferred because all necessary measurements can be performed from the central office. Consequently the capacity cannot be measured directly, but should be calculated through the estimation of the loop make-up. This paper discusses some main difficulties of this identification. Moreover, in contrast to the traditional approach where the data are interpreted in the time domain, this paper presents a new approach by doing most of the processing in the frequency domain.

Keywords: Digital Subscriber Line (DSL), Single Ended Line Testing (SELT), transfer function estimation, channel capacity, loop qualification.

1 Introduction

When offering a digital subscriber line (DSL) subscription to a customer, the operator first needs to check whether this telephone line is physically capable of supporting the offered data rate. This is called 'loop qualification' and is different for each customer since it depends on the subscriber loop, i.e. the twisted pair cables connecting the customer premises to the central office. Many loop make-ups are possible, but typically a subscriber loop consists of a cascade of different cable sections with increasing diameter toward the customer.

The loop capacity could be measured directly with Dual Ended Line Testing (DELT) but this requires equipment at both line extremities. In contrast, with Single Ended Line Testing (SELT) all measurements are performed from the central office. This eliminates the necessity of dispatching a technician to the customer premises if no modem is present and this is the reason why SELT is gaining much attention lately. Unfortunately, the loop capacity cannot be measured directly from SELT data. The make-up of the subscriber loop has to be estimated first and from this, the transfer function can be found, from which we can then calculate the channel capacity estimation through Shannon's formula.

C. Wang (Ed.): AccessNets, LNICST 6, pp. 427–440, 2009.

Discovering information about the loop make-up through single ended line tests is possible with reflectometry. The basic principle is to inject an excitation signal in the subscriber loop under test, at the central office side. The signal propagates along the loop and each time it encounters an impedance discontinuity (gauge change, end of line,…) a part of the signal is reflected and travels back to the measuring instrument. Analyzing these reflections allows identifying the loop make-up. For more information on the kind of discontinuities and the uniqueness of their trace signature, the reader is referred to [1].

Despite the great benefits of single ended loop make-up estimation, there are few papers in literature addressing this problem. Most groups are researching the identification of the loop make-up, with capacity estimation as a possible application. However, an accurate estimate of the loop make-up is also a goal by itself, as it allows updating the loop records database which can be incomplete or inaccurate. Galli et al. [1], [2] use time domain reflectometry (TDR) with a square pulse as excitation signal and consequently the measured reflections are dependent on the shape of the injected pulse. Boets et al. therefore propose to use the one-port scattering parameter, which is the ratio of the reflected to the injected wave, as an indicator of the loop make-up [3],[4]. Here, the excitation signals are discrete multitones (DMT) placed on the ADSL frequency grid. Another measurement technique has been proposed by Dodds et al. [5], by energizing the line with a sinusoid with step-wise increasing frequency. The reflections are then received through coherent detection. Both latter measurement techniques can be catalogued as frequency domain reflectometry (FDR).

Independently of the chosen measurement technique, the collected reflections can be analyzed in the time domain or in the frequency domain. However, till now the identification of the loop make-up has mainly been attempted in the time domain [1]-[4]. In [5], Dodds et al. propose a frequency domain approach to bring out the position of the reflections. Unfortunately this is a non-parametric approach and as such human intervention is still needed to indicate which reflections are significant and to deduce the most probable loop make-up.

The aim of this paper is two-fold. Firstly, it discusses some of the main limitations one encounters when estimating the loop make-up of a subscriber loop and their effects on the existing techniques [1]-[5]. Secondly, it proposes a combination of the techniques mentioned above: the chosen measurement setup uses a DMT excitation as in [3], performs a first non-parametric estimation of the reflections in the frequency domain similar to [5] and finally uses a parametric estimator based on the models described in [4] to compute the most probable loop make-up. From this, the channel capacity can then be estimated.

The remainder of this paper is structured as follows. Section 2 provides the required mathematical background. Section 3 states the main encountered difficulties and physical limitations. Section 4 presents the proposed approach, focusing on the non-parametric estimation of the initial line lengths through frequency domain processing. Finally, Section 5 summarizes the most important conclusions.

2 Theoretical Background

Given that for single ended line measurements only the central office end of the line is accessible, the network should be considered as a one-port. All the information that

can be acquired about the network through this port is contained in the one-port scattering parameter $S_{11}(f)$, which is the ratio of the reflected voltage wave b to the incident voltage wave a. The one-port scattering parameter can easily be measured by means of a network analyzer in the frequency domain. If the telephone network consists of a single line, then this transmission line can be modeled as derived in [4].

$$S_{11}(f) = \frac{b}{a} = \frac{-\rho_g + \rho_l e^{-2\gamma L}}{1 - \rho_g \rho_l e^{-2\gamma L}} \tag{1}$$

L is the unknown length of the line, γ the propagation function of the line, ρ_l the reflection at the line end and ρ_g the reflection at the measurement device, as given by (2) and shown in Fig. 1.

$$\rho_l = \frac{Z_l - Z_c}{Z_l + Z_c};\ \ \rho_g = \frac{Z_g - Z_c}{Z_g + Z_c} \tag{2}$$

Z_l is the load at the line end, Z_c the characteristic impedance of the line and Z_g the impedance of the measurement device.

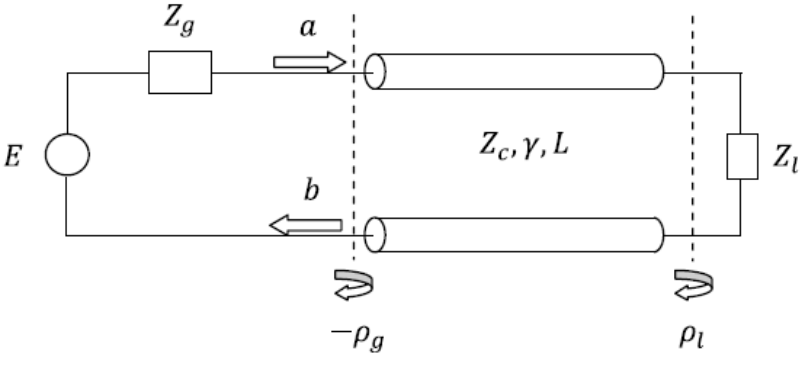

Fig. 1. Reflections for a subscriber loop consisting of a single line

If we linearize formula (1) according to:

$$\frac{1}{1+x} = 1 - x + x^2 - \cdots \qquad \text{for } |x| < 1$$

we obtain a structure which is straightforward to interpret.

$$S_{11}(f) = -\rho_g + \rho_l\left(1 - \rho_g^2\right)e^{-2\gamma L} + multiples\ . \tag{3}$$

The first term represents the reflection at the measurement device, due to the mismatch between the impedance of the measurement device and the characteristic impedance of the line. The second term is the reflection caused by the line end, which is the actual meaningful reflection containing information about the loop make-up. We will also receive multiples of this reflection because the signal bounces (in theory) infinitely back and forth on the line. In practice, however, the attenuation strongly increases with every multiple and as such only a few multiples (if any) will be visible.

We can rewrite (3) with the complex propagation function $\gamma = \alpha + j\beta$ and the following assumptions to keep the example simple without loss of generality: 1) we ignore the multiple reflections, 2) we neglect ρ_g^2 since a good measurement device will be approximately matched to the line under test, leading to a small ρ_g and a negligible ρ_g^2.

$$S_{11}(f) = -\rho_g + \rho_l e^{-2\propto L} e^{-2j\beta L} \tag{4}$$

In the general case, ρ_g and ρ_l are complex functions. We can write $S_{11}(f)$ in its complex notation:

$$\Re\{S_{11}(f)\} = -\Re\{\rho_g\} + e^{-2\propto L}[\Re\{\rho_l\}\cos(-2\beta L) - \Im\{\rho_l\} sin(-2\beta L)] \tag{5}$$

$$\Im\{S_{11}(f)\} = -\Im\{\rho_g\} + e^{-2\propto L}[\Re\{\rho_l\}\sin(-2\beta L) + \Im\{\rho_l\} cos(-2\beta L)] \ . \tag{6}$$

If the line end is open (as is the case for an on-hooked telephone), then $\rho_l = 1$ and the formulas reduce to:

$$\Re\{S_{11}(f)\} = -\Re\{\rho_g\} + e^{-2\propto L}\cos(-2\beta L) \tag{7}$$

$$\Im\{S_{11}(f)\} = -\Im\{\rho_g\} + e^{-2\propto L}\sin(-2\beta L) \ . \tag{8}$$

We will use these quantities in Section 4 to estimate the loop make-up.

Once the loop make-up has been estimated, the transfer function $H(f)$ can easily be calculated using the ABCD parameters [6]:

$$H(f) = \frac{Z_l(f)}{Z_g(f)\cdot[C(f)Z_l(f) + D(f)] + A(f)Z_l(f) + B(f)} . \tag{9}$$

Formula (10) gives the ABCD matrix for a single line [7].

$$\begin{pmatrix} A & B \\ C & D \end{pmatrix} = \begin{pmatrix} cosh(\gamma L) & Z_c sinh(\gamma L) \\ sinh(\gamma L)/Z_c & cosh(\gamma L) \end{pmatrix} . \tag{10}$$

The advantage of the ABCD matrix representation, is that for a cascade, the total ABCD matrix is simply the product of the individual ABCD matrices of the single lines.

The theoretical channel capacity of the subscriber line can then be calculated with Shannon's formula:

$$C = \int_{f_1}^{f_2} log_2\left(1 + \frac{|H(f)|^2 S(f)}{N(f)}\right) df \tag{11}$$

$N(f)$ is the power spectral density (PSD) of the noise, $S(f)$ is the PSD of the transmitted xDSL signal as defined by the standards [8], e.g. -40 dBm/Hz for ADSL downstream, and $[f_1, f_2]$ is the frequency band in which the xDSL service operates.

3 Difficulties

This section discusses some main difficulties one encounters when attempting to estimate the loop make-up of a subscriber loop from single ended line tests. We will illustrate them in the simplest case, namely a single line, with the line length L as the unknown parameter. The described problems are independent of the chosen measurement domain, so they occur with TDR as well as FDR.

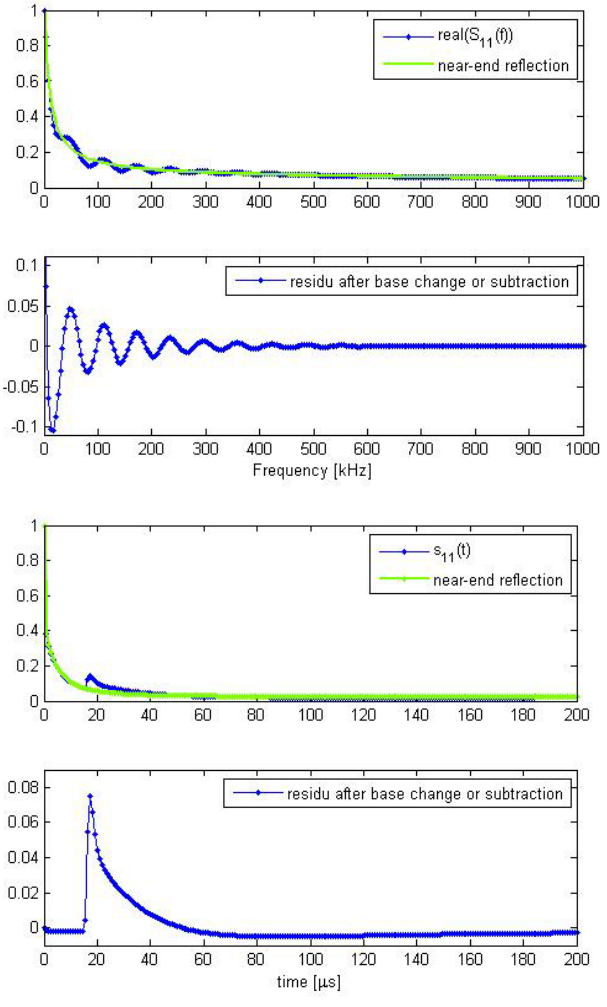

Fig. 2. Near-end reflection partially masking the line end reflection of a 1800 m line; when removing the near-end reflection the end reflection becomes more clearly visible; frequency domain (*top*), time domain (*bottom*)

3.1 Near-End Reflection

The first problem we encounter is the unwanted reflection ρ_g at the measurement device, because the measurement device can never perfectly be matched to the line under test. This impedance mismatch causes a reflection, called the 'near-end' reflection (first term in (7) and (8)), which can partially or totally mask the reflections of interest [1],[3]. Fig. 2 illustrates this problem for a single line of 1800 m.

Several approaches are possible to tackle this problem. In [3] the chosen impedance in which the measured scattering parameter is expressed is changed, as to match the characteristic impedance of the line as well as possible ($Z_{new} \approx Z_c$). This is done through post-processing with (12). This implies that the characteristic impedance of the line needs to be estimated first using a parametric model.

$$S_{11,new} = \frac{Z_g\left(\frac{1+S_{11}}{1-S_{11}}\right) - Z_{new}}{Z_g\left(\frac{1+S_{11}}{1-S_{11}}\right) + Z_{new}}. \tag{12}$$

In [1] and [5] the near-end reflection ρ_g is estimated by measuring a very long line, in the time and frequency domain respectively. The near-end reflection is then subtracted from the measured data. However, this assumes that a very long line is available. A third possibility is fitting the near-end reflection. In [9] a rational function of second order over first order in the frequency domain was found to give satisfactory results.

In any case, it is important to reduce the near-end reflection as much as possible, to ease the identification of the loop make-up.

3.2 Dispersion

If the near-end reflection can be completely removed, formulas (7) and (8) further simplify to:

$$\Re\{S_{11}(f)\} = e^{-2\propto(f)L}\cos(-2\beta(f)L) \tag{13}$$

$$\Im\{S_{11}(f)\} = e^{-2\propto(f)L}\sin(-2\beta(f)L)\,. \tag{14}$$

Note that the frequency dependence has been mentioned explicitly in these expressions. If the phase constant β would be a linear function of the frequency ($\beta = m \cdot f$ with $m \in \mathbb{R}$), an inverse Fourier transform of the sinusoidal term would yield a Dirac pulse at time mL/π. This can then be related to the unknown line length L through the propagation velocity v_p. In practice, β is almost a linear function of frequency and as a consequence we have a lobe around the exact spatial location instead of a Dirac pulse. In the time domain, this phenomenon manifests itself as dispersion due to the fact that the propagation velocity is slightly frequency dependent. The propagation velocity v_p is related to β as follows:

$$v_p(f) = \frac{2\pi f}{\beta(f)}\,. \tag{15}$$

Moreover, the exponential term will widen the reflection even further. The fact that the attenuation constant α is not a constant, in contrast to what its name suggests, causes supplementary dispersion in the time domain.

As a consequence, in the time domain the reflections show long tails due to the dispersive nature of twisted pairs. This can already be seen in Fig. 2 for a single line. When the loop consists of a cascade of line segments, each k-th reflection r_k will be superimposed on the tail of the preceding reflections r_{k-1}, r_{k-2},…, r_1, as such distorting the isolated shape of the individual reflections (see Fig. 3). This complicates the feature extraction and models are needed to take into account the effects of this superposition [10].

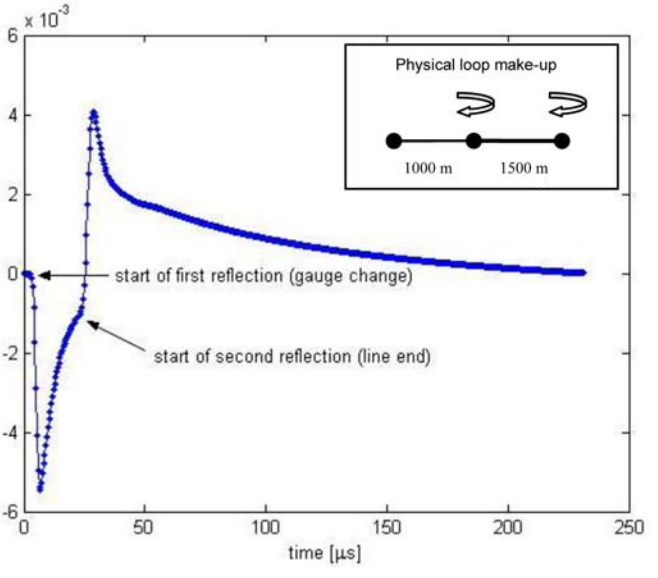

Fig. 3. Due to dispersion, the second reflection is superposed on the tail of the first reflection. This blurs the precise start of the second reflection.

3.3 Spatial Resolution

Fig. 4 shows a typical setup at the central office. The voice signals of the Plain Old Telephony Service (POTS) and the data from the xDSL are separated through a splitter. If the measurement device can be placed between the splitter and the Main Distribution Frame, then the whole frequency band can be measured. However, this is often not possible (e.g. for competitive local exchange carriers) and the measurement device will more probably be placed in the Digital Subscriber Line Access Multiplexer (DSLAM). As a consequence, for test purposes, the low frequencies will be missing or distorted.

Besides the problem of the missing low frequencies, which fixes the minimal usable frequency, in real measurements the maximal frequency is also bounded by practical implementation issues. First of all, the maximal frequency is described in the standards of the considered xDSL technology and sending energy outside this band is

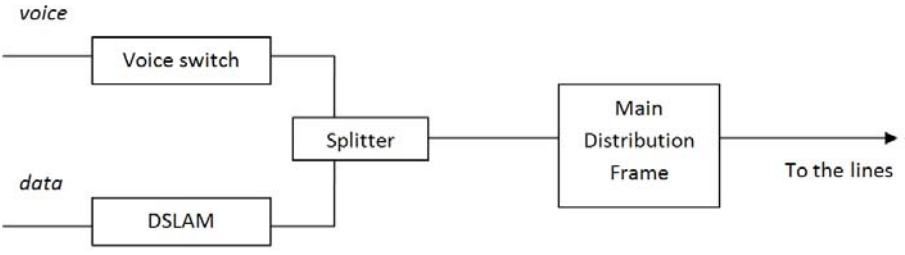

Fig. 4. Splitting of voice and data at the central office

not allowed. Moreover, the signal-to-noise ratio also constrains the maximal usable frequency, as the one-port scattering parameter decreases exponentially. Furthermore, the reliability of some frequencies might be insufficient for other reasons, e.g. distortions due to the nonlinear balun behavior at low frequencies.

As a consequence of these distorted frequencies, the TDR trace will be altered as well. By way of contrast, in the frequency domain only a few data points will be missing or distorted. Therefore, in the frequency domain, the used frequency band can be chosen as to take only the unaffected frequencies into account. This is a main advantage of FDR.

Anyhow, only a part of the measured frequency band will be reliable and should be used for identification. As the spatial precision is inversely proportional to the used frequency band (see 16), a high f_{max} is desired to be able to resolve close discontinuities. On the other hand, (17) illustrates that the maximal resolvable distance is inversely proportional to the frequency grid Δf. For ADSL, the frequency grid consists of multiples of 4312.5 Hz, which leads to a maximal resolvable distance of 11.5 km, which is sufficient for xDSL applications.

$$t_{precision} = \frac{1}{f_{max} - f_{min}}\,;\; L_{precision} = \left(\frac{1}{f_{max} - f_{min}}\right)\frac{v_p}{2} \tag{16}$$

$$t_{max} = \frac{1}{2\Delta f}\,; \qquad L_{max} = \left(\frac{1}{2\Delta f}\right)\frac{v_p}{2} \tag{17}$$

In practical situations, the usable frequency band might be quite small. If, for example the voice band signals are suppressed by the splitter ($f_{min} = 25\ kHz$) and the maximal frequency $f_{max} = 600\ kHz$, this gives a spatial precision of $175\ m$, which is often insufficient. If the maximal frequency cannot be increased any further, then zero padding can be a solution by artificially extending the data sequence with zeroes. Fig. 5 shows a simulation example: a 1200 m 0.4 mm line cascaded with a 400 m 0.5 mm line. When the data record is not extended by increasing f_{max} or by zero padding, then the two reflections cannot be resolved.

A good resolution and peak separation in the time domain are highly desired for good loop make-up estimation and zero padding can help in achieving this goal. However, it must be mentioned that zero padding also introduces small side lobes in the spectrum. Fortunately, the amplitudes of the side lobes are normally small enough not to be mistaken for a reflection.

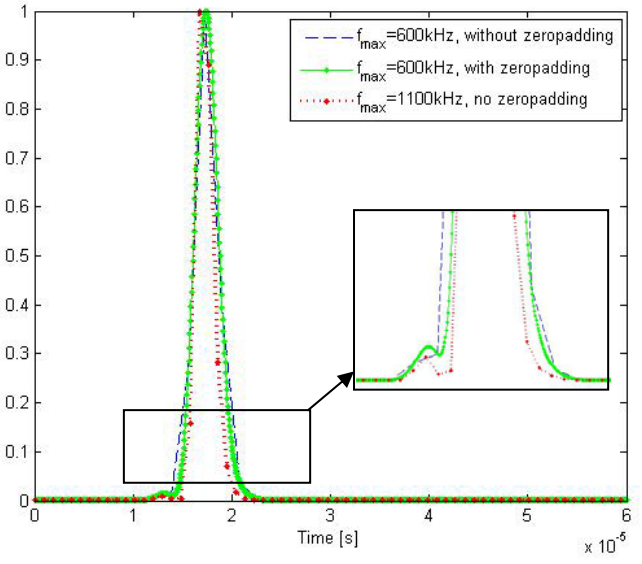

Fig. 5. A 1200 m 0.4 mm line cascaded with a 400 m 0.5 mm line. The time precision can be improved by increasing f_{max} (often not possible in practice) or zero padding.

4 Proposed Approach

As mentioned in the introduction, up till now the processing and identification have mainly been done in the time domain. This has the advantage of being straightforward to understand, as each peak (e.g. Fig. 3) corresponds to the reflection one receives when exciting the line with a pulse. When using TDR as in [1], the reflectogram is measured directly in the time domain. In contrast, in [3] the one-port scattering parameter is measured in the frequency domain and then transformed to the time domain through an ifft. The signal is then processed in the time domain to visualize the reflection information as clearly as possible. This then corresponds to the impulse response of the line, similar to TDR.

We use the same setup as in [3], but instead of transforming the measured one-port scattering parameter into the time domain to analyze it there, we propose to do some processing in the frequency domain first, like in [5]. The main concept is to exploit the information in the periodicity of $S_{11}(f)$ (see Fig. 2.), generated by the standing waves caused by the reflections on the loop. Only after this processing, will the inverse Fourier transform (ifft) be used to return to the time domain, to relate the reflections to line lengths. Finally, a parametric optimization is performed in the frequency domain, based on the models from [4], to obtain the final estimate of the loop make-up.

The one-port scattering parameter is processed in the following way:

- the complex representation is used;
- the near-end reflection is removed;
- the signal is windowed;

- only the reliable frequency band is taken into account;
- the signal is zero padded.

We will now motivate the purpose of each of these processing steps.

4.1 Processing

Complex Representation

A complex quantity, like the one-port scattering parameter is most often expressed in its polar representation. In the case of a single line, the one-port scattering parameter is given by:

$$|S_{11}(f)| = \sqrt{\begin{matrix}|\rho_g|^2 + e^{-4\propto L} - \\ 2e^{-2\propto L}\left[\Re\{\rho_g\}\cos(-2\beta L) + \Im\{\rho_g\}\sin(-2\beta L)\right]\end{matrix}} \tag{18}$$

$$\angle S_{11}(f) = Bgtg\left(\frac{-\Im\{\rho_g\} + e^{-2\propto L}\sin(-2\beta L)}{-\Re\{\rho_g\} + e^{-2\propto L}\cos(-2\beta L)}\right). \tag{19}$$

The magnitude of $S_{11}(f)$, as given by (18) is of the form $\sqrt{A + B\sin(x)}$. Using the series expansion:

$$\sqrt{1+z} = 1 + \frac{1}{2}z - \frac{1}{8}z^2 + \frac{1}{16}z^3 + \cdots$$

results in the following approximation:

$$\sqrt{A + \mathrm{Bsin}(x)} = \sqrt{A} + \frac{B}{2\sqrt{A}}\sin(x) - \frac{B^2}{8A\sqrt{A}}\sin^2(x) + \frac{B^3}{16A^2\sqrt{A}}\sin^3(x) + \cdots \tag{20}$$

The first term is a DC component, the second term is the desired time component at $-2\beta L$ and the following terms give rise to harmonics. In theory the number of harmonics is infinite, however the amplitude quickly decreases. These harmonics are highly undesirable, as they complicate the analysis. In contrast, as one can see from (7) and (8), performing an ifft on the real or imaginary part, will bring out the present periodicities without harmonics. Therefore, we propose to work with the complex representation of $S_{11}(f)$, instead of the more classic polar representation.

The two top rows of Fig. 6 compare $S_{11}(f)$ in polar notation and complex notation for a 0.4 mm cable of 1000 m.

Near-End Reflection

The near-end reflection is removed by fitting it with a rational function of second order over first order [9]. The bottom row of Fig. 6 shows the residue after subtraction of the fit. The one-port scattering parameter $S_{11}(f)$ then reduces to an exponential damped sinusoid as given by (13)-(14).

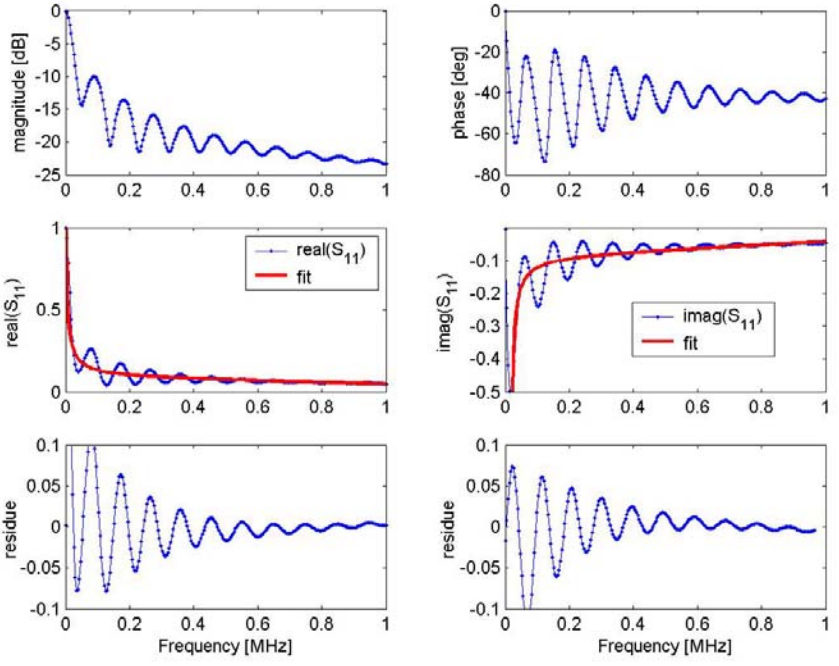

Fig. 6. $\boldsymbol{S_{11}(f)}$ represented in polar notation (*top*), $\boldsymbol{S_{11}(f)}$ represented in complex notation (*middle*) and $\boldsymbol{S_{11}(f)}$ in complex notation after base change or subtraction of fit (*bottom*) for a measured 1000 m segment of 0.4 mm

Windowing

From (13)-(14) we know that the signal is an exponentially damped sine, but the periodicity is unknown. Therefore, before applying the inverse Fourier transform to bring out the periodicities, the signal is windowed in order to avoid leakage. A Hanning window is used for this purpose as it was found to give good results. This windowing will further widen the reflection.

In summary, there are three contributions to the widening of the reflection in the time domain:

a) the propagation speed $v_p(f)$ is not a constant: this means that the sinusoidal function has a slightly changing periodicity;
b) the frequency dependent attenuation $e^{-2\propto(f)L}$;
c) the use of windowing: if no windowing is used, the reflection would be even wider due to leakage.

Reliable Frequency Band

As explained in section 3.C, the used frequency band should be chosen as large as possible, to have a good spatial resolution. On the other hand, unreliable frequencies

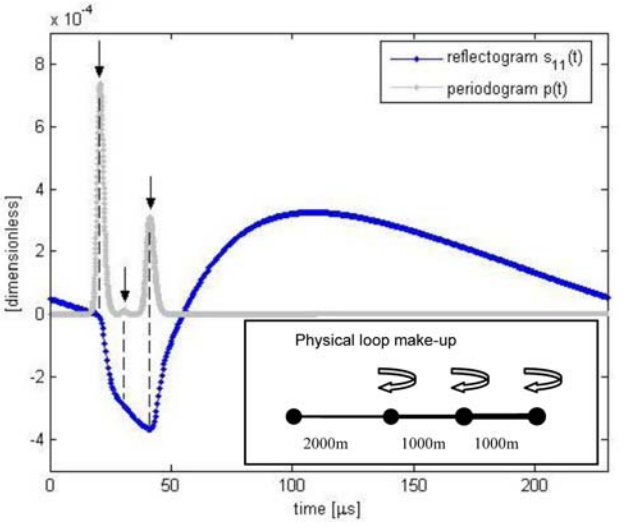

Fig. 7. Comparison between the reflectogram $\boldsymbol{s_{11}(t)}$ and the periodogram $\boldsymbol{p(t)}$ for a simulated cascade of 2000 m (0.4 mm), 1000 m (0.5 mm) and 1000 m (0.6 mm)

should not be taken into account. As such, a trade-off must be found between these two requirements. In the example of Fig. 7, the frequency band $[25{,}600]kHz$ was used.

Zero padding

In the example of Fig. 7 the reliable frequency band is small and as a consequence the number of remaining measurement points is low. Zero padding is used to improve the spatial resolution, as explained in section III.C. The length of the frequency signal is artificially tripled by adding twice as many zeroes as the length of the data.

4.2 Non-parametric Estimation

After all these operations, the periodogram of the processed signal is calculated:

$$p(t) = |ifft([S_{11}([f_1, f_2]) - fit; 0 \dots 0] \cdot hann)|^2 \,. \tag{21}$$

As a consequence, the signal is back in the time domain, but due to the executed manipulations, it has not the physical meaning of the reflectogram (impulse response) anymore. The new signal can be interpreted as a periodogram since it brings out peaks corresponding to each periodicity in $S_{11}(f)$ and each periodicity is generated by a change in the loop make-up. As such, the periodogram will have peaks corresponding to the reflections, just as in the reflectogram. However, due to the performed processing steps, the overlap of the reflections is strongly reduced.

In the case of a single line, there will be a one reflection after a time delay Δt, which can be converted to a line length L by using the propagation speed v_p of the cable:

$$L = \frac{v_p \Delta t}{2}. \tag{22}$$

Fig. 7 shows a more complicated example: a cascade of 2000 m (0.4 mm), 1000 m (0.5 mm) and 1000 m (0.6 mm). The reflectogram $s_{11}(t)$ and the periodogram $p(t)$ are compared. As one can see, the reflection overlap is strongly reduced with the proposed approach. As indicated by the arrows, the three reflections are now clearly separated in the periodogram, in contrast to the reflectogram where the start of the second reflection is very difficult to detect.

4.3 Parametric Estimation

Next, a reasoning system will analyze the periodogram to determine which reflections are genuine (due to the line end or gauge change) and which ones are multiple reflections or artificial reflections introduced by the processing. It does so by proposing several possible loop make-ups, calculating their periodogram and checking them against the periodogram of the measured subscriber loop.

The genuine reflections can then be translated to line lengths through (22). These lengths are used as initial line lengths for the non-linear optimization. Parametric models for $S_{11}^{mod}(f, \boldsymbol{P})$ are used as described in [4] and the following cost function is minimized:

$$C = \sum_{k=1}^{N} \frac{\left|S_{11}(f_k) - S_{11}^{mod}(f_k, \boldsymbol{P})\right|^2}{\sigma^2(f_k)} \,. \tag{23}$$

Once the loop make-up has been identified, the transfer function can be calculated with (9). The capacity of the subscriber line can then be estimated for a specific xDSL service with Shannon's formula (11).

5 Conclusions

This paper discussed some difficulties one encounters when identifying the loop make-up from single ended line measurements. Moreover, a new approach for the loop make-up identification by means of single ended line testing was proposed. The main difference with the literature is the domain in which the identification is performed. Till now the identification had mainly been attempted by analysis of the most important features of the reflectogram. This paper proposed a new approach by analyzing the features of another quantity, namely the periodogram of the measured one-port scattering parameter $S_{11}(f)$. The advantage is that the two main drawbacks of the time domain approach, namely dispersion and unreliable frequency bands are tackled. The reduced dispersion eases the loop make-up estimation, which positively affects the results of the estimated channel capacity. Moreover, the new algorithm uses only a chosen frequency band, which makes it unnecessary to by-pass the POTS-filter, which suppresses the voice-band in DSL operation. Once the loop make-up is estimated, the transfer function and the line capacity can be calculated. This is important for telephone companies providing DSL services, in order to have a tool to characterize and evaluate the capability of a subscriber local loop in carrying DSL services.

References

1. Galli, S., Waring, D.L.: Loop Makeup Identification Via Single Ended Testing: Beyond Mere Loop Qualification. IEEE J. Sel. Areas Commun. 20(5), 923–935 (2002)
2. Galli, S., Kerpez, K.J.: Single-Ended Loop Make-Up Identification. IEEE Trans. Instrum. Meas. 55(2), 528–549 (2006)
3. Boets, P., Bostoen, T., Van Biesen, L., Pollet, T.: Pre-Processing of Signals for Single-Ended Subscriber Line Testing. IEEE Trans. Instrum. Meas. 55(5), 1509–1518 (2006)
4. Bostoen, T., Boets, P., Zekri, M., Van Biesen, L., Pollet, T., Rabijns, D.: Estimation of the Transfer Function of a Subscriber Loop by Means of One-Port Scattering Parameter Measurement at the Central Office. IEEE J. Sel. Areas in Commun. 20(5), 936–948 (2002)
5. Celaya, B., Dodds, D.: Single-Ended DSL Line Tester. In: Proc. Canadian Conf. on Electrical and Computer Engineering, pp. 2155–2158 (2004)
6. Chen, W.Y.: DSL: Simulation Techniques and Standards Development for Digital Subscriber Line Systems. MacMillan Technical Publishing, U.S.A (1998)
7. Starr, T., Cioffi, J., Silverman, P.: Understanding Digital Subscriber Line Technology. Prentice Hall, New Jersey (1999)
8. Asymmetric digital subscriber line (ADSL) transceivers. ITU, Recommendation G.992.1 (1999)
9. Neus, C., Boets, P., Van Biesen, L.: Transfer Function Estimation of Digital Subscriber Lines. In: IEEE Proc. Instrum. Meas. Techn. Conf. 1–5 (2007)
10. Vermeiren, T., Bostoen, T., Louage, F., Boets, P., Chehab, X.O.: Subscriber Loop Topology Classification by means of Time Domain Reflectometry. In: Proc. IEEE Int. Conf. Comm, pp. 1998–2002 (2003)